Organic & Biomolecular Chemistry

Cite this: *Org. Biomol. Chem.*, 2012, **10**, 3288

www.rsc.org/obc

PAPER

Synthesis and evaluation of novel aza-caged *Garcinia* xanthones†

Xiaojin Zhang,‡[a] Xiang Li,‡[a] Haopeng Sun,*[b] Zhengyu Jiang,[b] Lei Tao,[c] Yuan Gao,[c] Qinglong Guo*[c] and Qidong You*[a,c]

Received 13th December 2011, Accepted 13th February 2012
DOI: 10.1039/c2ob07088j

Inspired by the therapeutic potential of the simplified caged xanthones, we have developed a chemical strategy for synthesizing novel aza-caged *Garcinia* analogues through a regioselective Claisen/Diels–Alder cascade reaction. The origin of regioselectivity has been explained using the DFT method. We have further evaluated the cell proliferation and IKKβ inhibitory activities of these compounds and studied their binding mode with IKKβ by molecular docking. The results suggested that the aza-caged scaffold provides a suitable modification site and the introduction of a hydrophobic moiety leads to improvement in the cytotoxicity and IKKβ inhibitory activity. The aza-caged compound **6c** exhibited an IC_{50} value of 2.68, 2.10, 8.02 μM against the HepG2, A549 cells and IKKβ, respectively. Mechanism studies with **6c** showed that the aza-caged compounds induce apoptosis and cell cycle S phase arrest in A549 cells.

Introduction

Gamboge, the resin collected from the tropical trees of the genus *Garcinia*, has been used as folk medicine for centuries in Southeast Asia.[1] Efforts to identify the bioactive constituents of gambogin have yielded a growing family of natural products defined as "caged xanthones", the structure features of which share an intriguing 4-oxa-tricyclo[4.3.1.$0^{3,7}$]dec-8-en-2-one scaffold merged into a common xanthone backbone.[2] Among these caged *Garcinia* xanthones, gambogic acid (GA, **1**) (Fig. 1) is the most prominent and representative example. Preclinical investigation demonstrated that **1** possessed potent anti-tumor activity both *in vitro* and *in vivo* and displayed an appropriate therapeutic window for clinical applications as an anti-cancer agent.[3] Practically, the gambogic acid injection has recently finished phase II clinical trials in cancer patients in China.[4]

The significant anti-tumor activity of **1** has attracted increasing worldwide research interest. Biological studies revealed that the anti-tumor efficacy of **1** arose through multiple mechanisms, including apoptosis induction,[5] cell cycle regulation,[6] anti-angiogenesis,[7] tumor cell adhesion inhibition *etc.*[8] Wang *et al.* reported a comprehensive proteome profiling which deduced stathmin 1 (STMN1) as the target of **1**.[9] In addition, the surface plasmon resonance studies showed that **1** bound to the N-terminal domain of heat shock protein 90 (Hsp90).[10] Another study showed that **1** inhibited the nuclear factor-κB (NF-κB) signaling pathway[11] and induced apoptosis through its interaction with the transferrin receptor.[12] Meanwhile, interaction studies using biotin labeled GA suggested that **1** covalently bound to IκBα kinase-β (IKKβ) protein through the oxa-caged moiety as a bioactive Michael acceptor and thus suppressed NF-κB activation.[13]

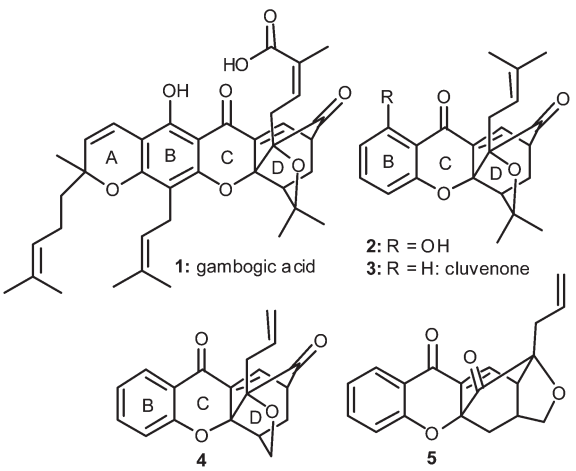

Fig. 1 Chemical structures of selected caged *Garcinia* xanthones and analogues.

[a]*State Key Laboratory of Natural Medicines (China Pharmaceutical University), Nanjing, 210009, China. E-mail: youqidong@gmail.com; Tel: +86-25-83271351*
[b]*Department of Medicinal Chemistry, School of Pharmacy, China Pharmaceutical University, Nanjing, 210009, China. E-mail: sunhaopeng@163.com; Tel: +86-25-83271216*
[c]*Jiangsu Key Laboratory of Carcinogenesis and Intervention, China Pharmaceutical University, Nanjing, 210009, China. E-mail: anticancerdrug@yahoo.cn; Tel: +86-25-83271440*

†Electronic supplementary information (ESI) available: Experimental procedures for **3–5**, ^{1}H and ^{13}C NMR spectra for **11**, **12**, **13**, **8**, **7**, **14**, **17**, **20a–e**, **6a–e**. ^{1}H-^{1}H COSY, HSQC, HMBC spectra for **6a**, **17**. Energy data for **7**, **15–17**, **20a–23a**, **6a**, **25–27**, **4–5**. See DOI: 10.1039/c2ob07088j

‡These two authors contributed equally to this work.

Our recent studies further verified that IKKβ was the key regulator of the NF-κB pathway affected by **1**.

Previous SAR studies indicated that the whole A ring moiety and the carboxyl group of **1** could be removed thoroughly without obvious loss of anti-tumor potency, while the intact BCD ring containing the D-ring caged scaffold was the minimum pharmacophoric motif that essential for its activity.[14,15] Recently, several simplified analogues were reported to maintain the cytotoxicity exhibited by GA. For example, compound **2** displayed comparable activity to GA (**1**) against BGC-823 (gastric carcinoma) and HepG2 (hepatocellular carcinoma) cells at the low micromolar levels.[14] Cluvenone (**3**) was also reported to possess similar activity to GA (**1**) against HL-60 (promyelocytic leukemia) and HL-60/ADR cells with an IC_{50} value of 1.5 and 1.4 μM respectively.[15,16] Furthermore, compound **4** with remarkable simple structure was still found to have GI_{50} values of 1–2 μM in T47D (breast cancer), HCT116 (colon cancer) and SNU398 (hepatocellular carcinoma) cells and to be about 10–15 fold less active than GA (**1**).[17]

These caged analogues could be expediently obtained utilizing a Claisen/Diels–Alder cascade reaction from their bis-allyloxy precursors.[18] However, in the pursuit of greatly simplified analogues such as **3** and **4**, the initial non-regioselective Claisen rearrangement led to the formation of the regular oxa-caged scaffold as well as a neo caged scaffold as in **5**.[14,16–17] The resulting mixture of isomers shared similar properties and brought great difficulties in separation. Moreover, current synthetic strategies were limited in providing the oxa-caged scaffold,[18,19] whereas the oxa-caged moiety as in **4** lacked the suitable modification sites to help to further understand the surrounding SAR and improve the drug-like properties. Therefore, we sought to replace the oxygen atom in the caged scaffold by a sp^3 hybridized nitrogen atom to provide another modification site as shown in Fig. 2. Herein, we present a regioselective chemical strategy that allows to the synthesis of novel aza-caged *Garcinia* analogues with the 4-aza-tricyclo[4.3.1.$0^{3,7}$]dec-8-en-2-one scaffold and their biological evaluation.

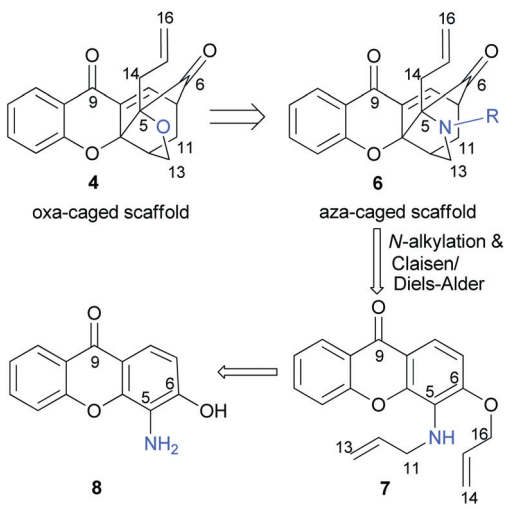

Fig. 2 Design of aza-caged *Garcinia* analogues and the synthetic approach.

Results and discussion

Synthesis of aza-caged *Garcinia* xanthones and study on the regioselective Claisen/Diels–Alder cascade reaction

Inspired by the synthesis of oxa-caged xanthones, our initial synthetic approach toward aza-caged scaffold is shown in Fig. 2. We expected aza-caged scaffold **6** to arise from regioselective Claisen/Diels–Alder cascade reaction of precursor **7** followed by a simple *N*-alkylation, the aza-caged ring system of which can be traced to xanthone **8** that substituted with amino and hydroxyl groups. With this in mind, our synthetic studies commenced with a $ZnCl_2$-mediated condensation of salicylic acid (**9**) with resorcinol (**10**) in $POCl_3$ to produce benzophenol adduct **11** in 72% yield. Initial efforts to convert **11** into xanthone **12** were using a conventional thermal method by refluxing benzophenol **11** in water with NaOAc as a base catalyst. Nevertheless, only 8% conversion was observed upon refluxing for 24 h. On account of the advantages of microwave irradiation (MWI) in accelerating organic reactions,[20] we tested this cyclization reaction under MWI using the same reaction system and found that **12** could be successfully obtained in short time in quantitative yield. The introduction of an amino group at C5 position was accomplished by a two step procedure that involved nitration of **12** to form **13** followed by reduction of the nitro group to provide **8** (57% combined yield). Subsequently, xanthone **8** was allylated with allyl chloride in the presence of K_2CO_3 to afford the desired di-allylated product **7** in 38% yield together with the mono- and tri-allylated products **14** and **20b** (93% yield in total) (Scheme 1).

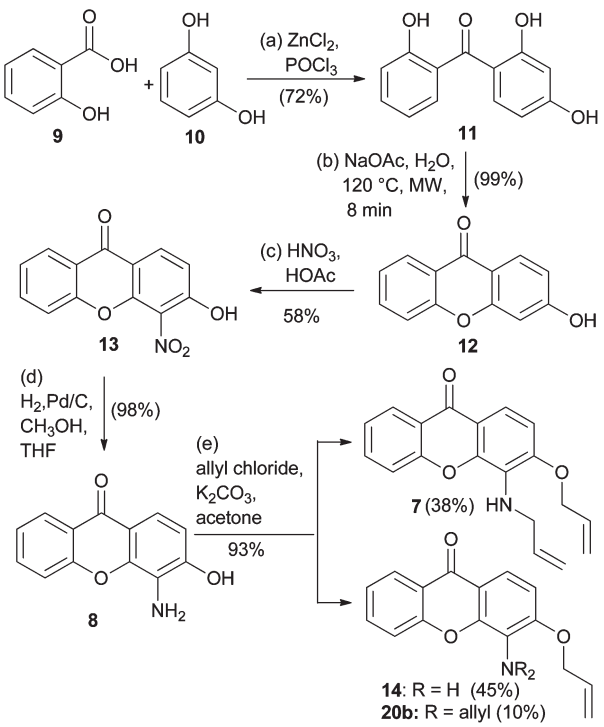

Scheme 1 *Reagents and conditions*: (a) $ZnCl_2$, $POCl_3$, 68 °C, 2 h, 71%; (b) 0.1 equiv. of NaOAc, H_2O, MWI (120 °C, 150 W), 8 min, 99%; (c) HNO_3, HOAc, 60 °C, 20 min, 58%; (d) H_2, Pd/C, CH_3OH–THF 1 : 1, 25 °C, 3 h, 98%; (e) K_2CO_3, allyl chloride, acetone, 45 °C, 1 h, **7** (38%), **14** (45%) and **20b** (10%).

With the cascade precursor **7** in hand, the stage was set to study the proposed Claisen/Diels–Alder reaction to construct the designed aza-caged scaffold. Drawing on previous experience with related substrates,[21] we heated compound **7** in decalin at 180 °C with attempt to produce the regular aza-caged product **18** and its probable isomer **19** (or ketone **5** that likely formed upon imine hydrolysis of **19**) (Scheme 2). This reaction afforded an unexpected product **17** in 58% yield with 33% recovery of **7**. None of the probable caged structures were isolated. By comparing the structure of reactant **7** and product **17**, it was supposed that **17** was formed through a rearrangement involving the C16 allyl group migration from the C6 oxygen to the C5 nitrogen of **7**.

Why did the reaction proceed through C5 nitrogen allylation? The answer may lie in the potential intramolecular hydrogen bond between C6 oxygen and C5 amino group in precursor **7**. The hydrogen bond could accept electron density from the C6 oxygen atom. This contributed to a weakening of the ether bond to the C16 allyl fragment. In addition, the C9 carbonyl group of precursor **7** was *para* to the C6 allyloxy unit and this also facilitated the rupture of the C16 allyl group. We proposed that precursor **7** was prone to undergoing a hydrogen bond mediated six-membered ring transition state as shown in path C (Scheme 2). While the C16 allyl group migrated to the C5 nitrogen, the hydrogen on the C5 amino group shifted simultaneously onto the C6 oxygen atom. Notably, the hydrogen bond and aromaticity of the xanthone ring were highly retained during the process from precursor **7** to product **17** by path C. However, in the case of the non-observed Claisen rearrangement pathway (path A and B), the states of the C5 or C6 atom changed from sp^2 hybridization in **7** into sp^3 hybridization in **15** and **16**. This led to the destruction of the intramolecular hydrogen bond and aromaticity of xanthone ring. As a result, both paths A and B needed much more extra energy compared with path C. In addition, molecular energies of the potential allyl rearrangement products were further evaluated by the DFT (density functional theory) method at the B3LYP/6-31G(d) level, computed using Gaussian 03.[22] The results were consistent with the above speculation, and the calculated energies (relative to precursor **7**) were 21.0, 33.8 and 0.5 kcal mol^{-1} for compounds **15**, **16** and **17**, respectively.

Realizing the problem encountered, we decided to first alkylate the C5 amino group to eliminate the effect of hydrogen bond and then perform the cascade reaction. As shown in Scheme 3, compound **7** was first treated with methyl iodide in the presence of K_2CO_3 to give precursor **20a** in 99% yield. Encouragingly, heating precursor **20a** in decalin at 180 °C for 3 h successfully furnished the desired aza-caged product **6a** in 53% yield with 36% recovery of **20a**. The structure of **6a** was further confirmed by two-dimensional correlation NMR spectroscopy. Since substrate **20a** without intramolecular hydrogen bonding could successfully afford the caged scaffold, it was verified again that the intramolecular hydrogen bond played an important role in hindering the Claisen/Diels–Alder reaction in substrate **7**.

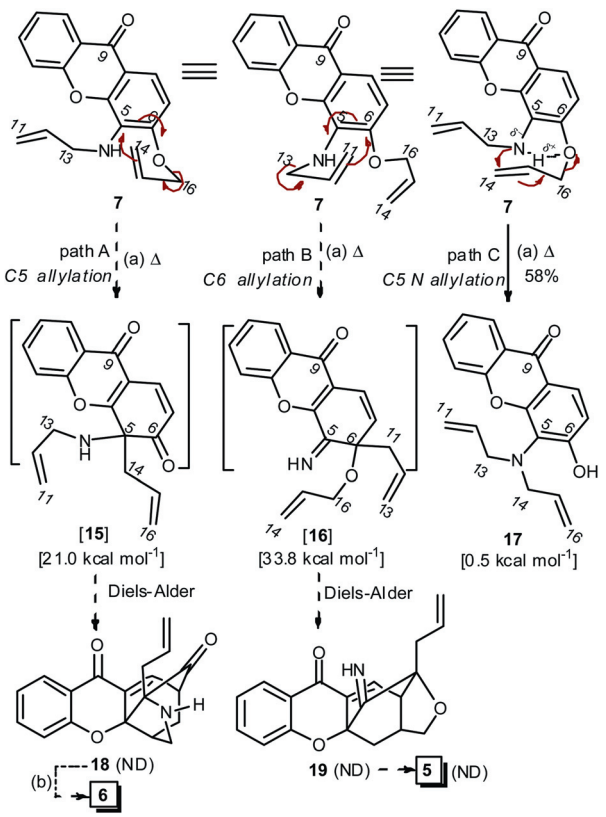

Scheme 2 *Reagents and conditions*: (a) decalin, 180 °C, 3 h, 58%; (b) RX, K_2CO_3, acetone. Energies given in square brackets are differences of energies relative to precursor **7**.

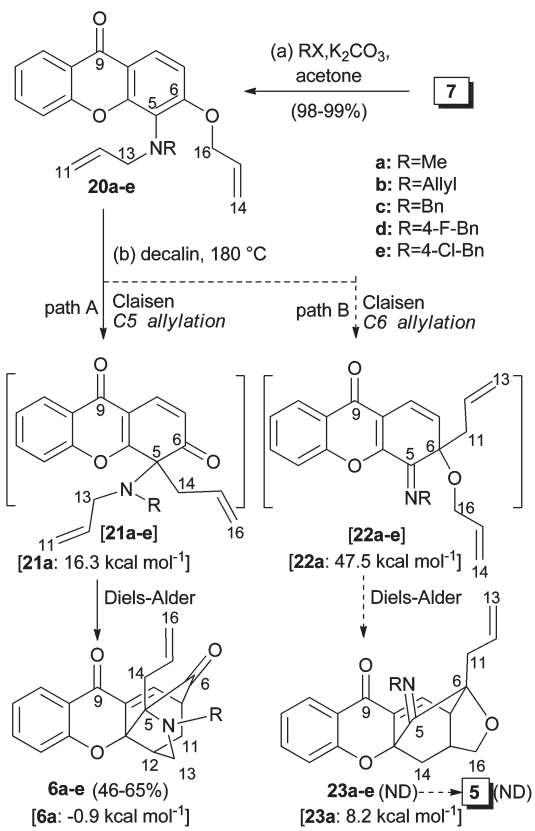

Scheme 3 *Reagents and conditions*: (a) K_2CO_3, acetone, 25 °C, overnight, 98–99%; (b) decalin, 180 °C, 3 h, 46–65%. Energies given in square brackets are the differences in energies relative to precursor **20a**.

In a similar manner, treating compound **7** with different alkylating agents afforded substrates **20b–e** in 98–99% yields with different substituents including allyl, benzyl and substituted benzyl groups. These substrates were selected to further test the cascade reaction and to tentatively detect the volume of the binding pocket around the caged region. Substrates **20b–e** were then subjected to the same reaction conditions and gave rise to the regular aza-caged compounds **6b–e** as expected in 46–65% yields with about 30% recovery of substrates **20b–e**. Importantly, we were not able to isolate any products containing the possible neo caged scaffold as in compounds **23a–e** or compound **5** that could likely be formed upon imine hydrolysis of **23a–e**. These results suggested that the amino-xanthone precursors **20a–e** with a C–N bond at C5 position could engage in a regioselective Claisen rearrangement pathway by the C5 allylation (A, Scheme 3) to furnish the intermediates **21a–e**. The intermediates could then undergo intramolecular Diels–Alder reactions to provide the designed regular caged analogues **6a–e** selectively.

For comparison purpose, the precursor **25** with a C–O bond at C5 position was synthesized by allylation of xanthone **24** (Scheme 4). Compound **24** was conveniently obtained according to the method reported previously.[15] When the dialloxy substituted precursor **25** was exposed to similar reaction conditions, it produced the regular caged scaffold **4** together with the neo scaffold isomer **5** in a ratio of about 1 : 1 with a combined yield of 61%. In this case, the precursor **25** ought to undergo an initial non-regioselective Claisen rearrangement pathway through both the C5 and C6 allylation (A, B, Scheme 4) and followed by the Diels–Alder addition.

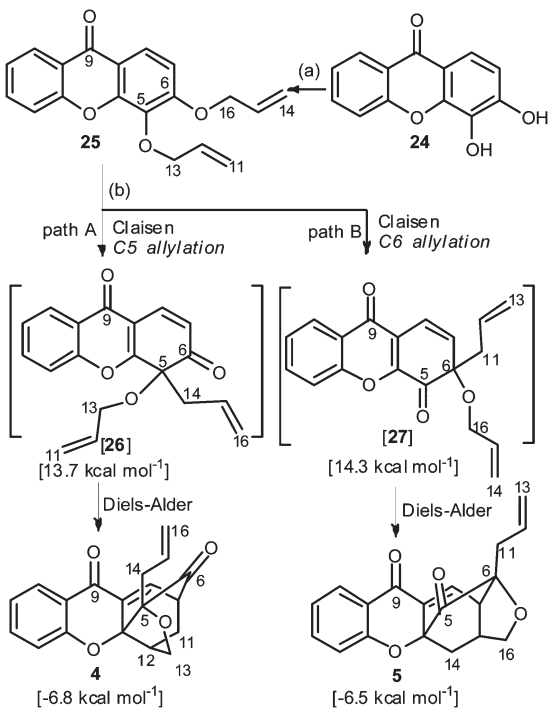

Scheme 4 *Reagents and conditions*: (a) K_2CO_3, allyl chloride, DMF, 45 °C, 2 h, (b) decalin, 180 °C, 3 h, **4** (32%) and **5** (29%). Energies given in square brackets are the differences in energies relative to precursor **7**.

Why was the Claisen/Diels–Alder reaction regioselective in precursors **20a–e** but non-regioselective in the case of precursor **25**? We supposed that this phenomenon was mainly due to the energy differences between the Claisen products by path A and path B. In the case of precursors **20a–e** (Scheme 3), comparing the two type of Claisen products **21a–e** by path A and **22a–e** by path B, the former possessed a C–N single bond at C5 and a C═O double bond at C6 while the latter had a C═N double bond and a C–O single bond at corresponding positions. According to references,[23] the general bond energies of C–N, C═O, C–O and C═N were about 73, 191, 86 and 147 kcal mol^{-1}, respectively. From this point of view, the energy of **21a–e** was greatly lower than **22a–e** (about −31 kcal mol^{-1}), which led to the selectivity in the initial Claisen rearrangement. While in the case of precursor **25** (Scheme 4), the similar bonds in the two type of Claisen products **26** and **27** resulted in similar molecular energies. Furthermore, to confirm the above assumptions, we selected precursors **20a** and **25** as representatives and calculated the molecular energies of their rearrangement products by DFT method. The results revealed that the energy differences between **21a**/**22a** and **26**/**27** were −31.2 and −0.6 kcal mol^{-1}. Moreover, a large energy differences were also observed between the pair of caged moieties (−9.1 kcal mol^{-1} for **6a**/**6a** and −0.3 kcal mol^{-1} for **4**/**5**). These findings could explain the different selectivity between **20a–e** and **25** in the Claisen/Diels–Alder reaction.

Cell proliferation studies

The anti-proliferative activities of the synthesized caged *Garcinia* xanthone analogues were assessed by the tetrazolium-based MTT assay using human hepatocellular carcinoma HepG2 cell line, human lung carcinoma A549 cell line and human glioblastoma U251 cell line. Cancer cells were treated with increasing concentrations of the respective compounds for 24 h, and then the cell viability was evaluated through measurements of mitochondrial dehydrogenase activity. The anti-proliferative activities, expressed as IC_{50} values, were summarized in Table 1.

GA (**1**) was the most active compound among all the tested compounds and exhibited an IC_{50} value of 0.89, 1.10 and 2.56 μM against HepG2, A549 and U251 cells, respectively. All the analogues seemed to be less sensitive to U251 cells and showed moderate or even inactivity against U251 cells. The greatly simplified oxa-caged analogue **4** displayed relatively less potency than cluvenone (**3**). Importantly, all the aza-caged

Table 1 Inhibition of cell proliferation by caged *Garcinia* xanthones

	IC_{50}/μM		
Compound	HepG2	A549	U251
6a	10.9	6.84	16.7
6b	6.51	4.34	24.9
6c	2.68	2.10	16.4
6d	4.29	3.61	29.1
6e	3.89	5.02	26.2
4	16.7	18.9	>100
5	24.2	12.7	>100
Cluvenone (**3**)	6.77	1.93	18.7
GA (**1**)	0.89	1.10	2.56

compounds **6a–e** were found to be more active than the parent oxa-caged compound **4** against all the three cell lines. Furthermore, compounds **6c–e**, containing a relatively large volume of substituents, generally possessed a low micromolar activity ranging between 2.10 to 5.02 μM against HepG2 and A549 cells and were more potent than compounds **6a–b** with smaller groups. Especially, compound **6c**, the most potent compound among the aza-caged analogues, was almost 10 times more active than the parent oxa-caged compound **4** and two fold more potent than cluvenone (**3**) against HepG2 cells. These results suggest that: (a) the nitrogen atom of the 4-aza-tricyclo [4.3.1.$0^{3,7}$]dec-2-one caged scaffold is an accessible and suitable modification site to derive novel potential anti-tumor agents; (b) the introduction of hydrophobic moiety to the aza-caged region leads to an obvious increase in cytotoxicity as compared to the oxa-caged parent **4**; (c) the substituent groups with relative large volume are preferred during interacting with the putative receptor.

Table 2 The inhibition and binding information of GA and its analogues with IKKβ protein

Compound	IKKβ IC_{50}/μM	Gold score
6a	26.30	47.55
6b	19.80	49.78
6c	8.02	52.24
6d	10.12	52.77
6e	9.55	52.36
4	42.12	47.23
5	44.78	46.02
Cluvenone (**3**)	24.16	47.83
GA (**1**)	3.07	61.04

IKKβ inhibitory activity and binding pattern study by molecular docking

Since GA was reported to inhibit the activity of IKKβ,[13] a potential therapeutic target in cancer, we further tested the IKKβ inhibitory activity of these analogues by using HTScan IKKβ kinase assay kit. The IC_{50} values were summarized in Table 2. Among all the analogues, compound **6c** exhibited the most potent IKKβ inhibitory effect with an IC_{50} value of 8.02 μM. Although compound **6c** was less active than GA (**1**), it was about 3–5 times more effective than compound **4** and cluvenone (**3**). The trend observed in the IKKβ inhibition revealed to be consistent with the *in vitro* anti-tumor activity.

Recently, the crystal structure of IKKβ protein (PDB ID: 3DA8) has been reported by Xu's groups.[24] To further illustrate the binding mode of IKKβ with the caged compounds, a molecular docking study was performed using the protein (3DA8) and the program Gold 3.0. Goldscore Fitness was selected to evaluate the binding affinity (Table 2). By analyzing the data, it was evident that the values of the Goldscore Fitness were in correlation with the experimental IKKβ inhibitory activities, indicating that the docking model was reliable for the binding study. GA (**1**), the oxa-caged **4** and the aza-caged **6c** were taken as examples to depict the binding mode (Fig. 3). All the three compounds were located in the ATP binding pocket of IKKβ and possessed hydrogen bond with the hinge region of the enzyme, which was considered to be a common binding pattern of IKKβ inhibitors.[25] Specifically, compound **4** and **6c** formed a hydrogen bond with Cys99 and GA (**1**) formed a hydrogen bond with Gly102. There are mainly three important hydrophobic pockets (Fig. 3) in the binding site of IKKβ. P1 is formed by Leu21, Met96, Tyr98, Cys99, Val74, P2 is formed by Val152, Ile165 and Asn150, P3 is formed by Ile165, Asn150 and Gly22. As

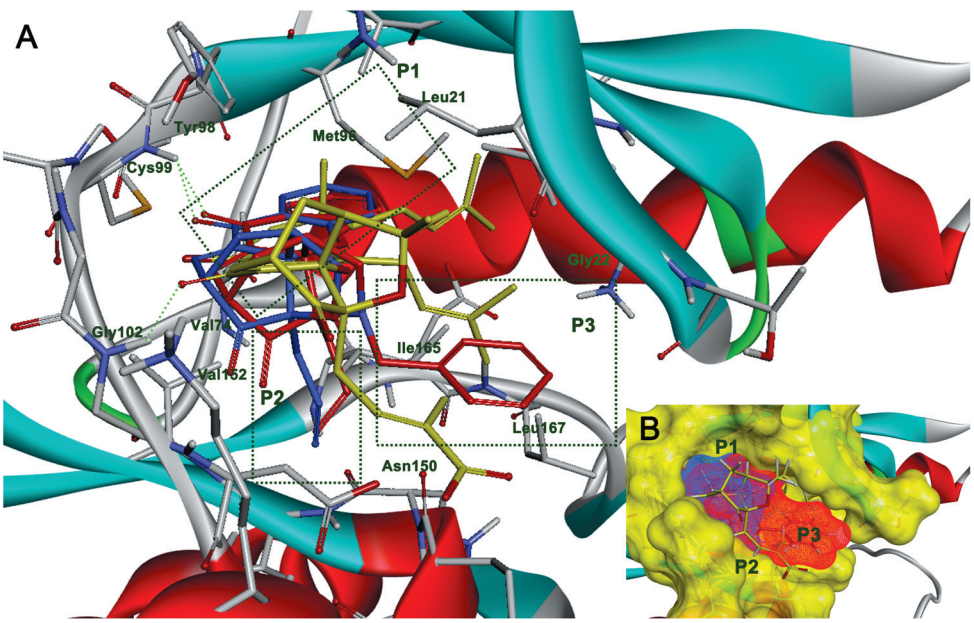

Fig. 3 (A) Molecular docking simulations for GA (**1**) (yellow), **4** (blue) and **6c** (red). Residues in the binding pocket were shown as gray sticks. Hydrogen bonds were shown as green dotted lines; (B) solvent accessible surfaces of the binding pocket (solid, yellow), compound **4** (wire mesh, blue) and **6c** (wire mesh, red).

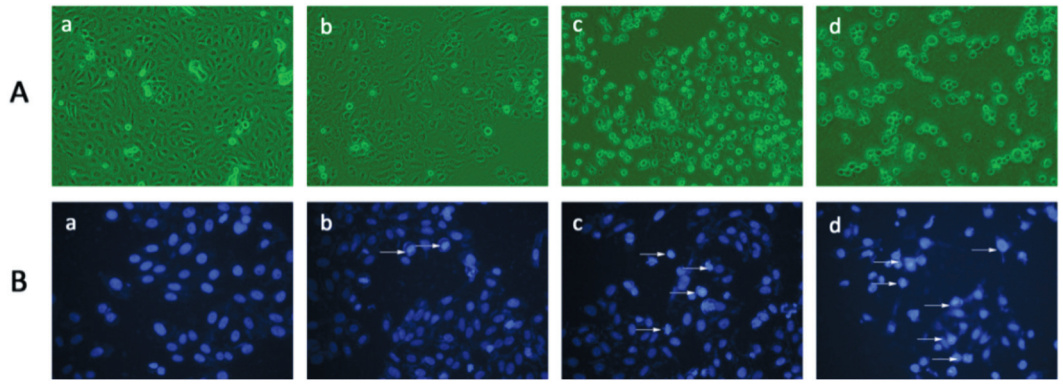

Fig. 4 Cell morphological assessment of **6c** on A549 cells. (A) Light microscopy detection (×200): (a) control group; (b) 2 μM of **6c**; (c) 4 μM of **6c**; (d) 8 μM of **6c**. (B) Fluorescence microscopy detection (×400): (a) control group; (b) 2 μM of **6c**; (c) 4 μM of **6c**; (d) 8 μM of **6c**. The white arrows point the observed apoptotic bodies.

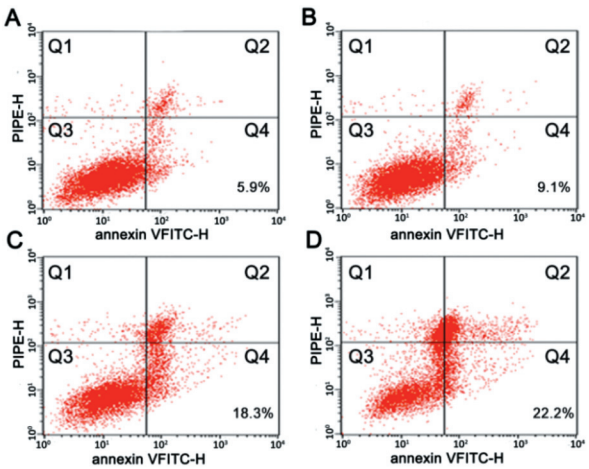

Fig. 5 Fluorescence-activated cell sorter analysis for **6c** on A549 cells by annexin-V/PI staining. Upper left: dead cells; upper right: late apoptotic cells; lower left: fully viable cells; lower right: early apoptotic cells. (A) Control group; (B) 2 μM of **6c**; (C) 4 μM of **6c**; (D) 8 μM of **6c**.

depicted in Fig. 3A, GA occupied all three hydrophobic pockets and especially fitted very well with the entail P1 pocket. Importantly, compound **6c** also possessed the three pockets but only inserted into the deep part of P1. However, compound **4** obviously missed the P3 pocket (Fig. 3B). These results explained the weak binding affinity for IKKβ of compound **4** and the significant increase of IKKβ activity and cytotoxicity of compound **6c** compared to **4**. The binding mode also revealed that there is an appropriate chemical modification space around the caged region as shown in P3 binding pocket.

Apoptosis and cell cycle distribution studies

To further study the mechanism of the aza-caged analogues, we selected the most active compound **6c** to study its effects on apoptosis and cell cycle distribution. Firstly, compound **6c** was evaluated for its influence on cell skeleton by a morphological observation study. The inverted light microscope (×200) demonstrated that incubation of 2 μM, 4 μM and 8 μM of compound **6c** for 24 h resulted in phenotypic changes of A549 cells, such as distortion, membrane blebbing and shrinkage, and a large proportion of cells became round in shape and underwent necrosis at high concentrations, while the untreated cells in the control group displayed a normal, healthy shape as shown by their clear cytoskeletons (Fig. 4). Significant morphological changes of early apoptosis were observed under the fluorescence microscope (×400) by DAPI staining (Fig. 5). Untreated A549 cells were stained uniformly and emitted blue fluorescence which indicated that the chromatin was equably distributed in the nucleolus. After treatment with compound **6c**, the bright nuclear condensation and the apoptotic bodies appeared as the key markers of cellular apoptosis. In detail, at 2 μM concentration, cell membrane still displayed integrity, and the nuclei exhibited bright condensed chromatin, at 4 μM and 8 μM concentration, typical apoptotic bodies and shrinkage were observed.

Subsequently, the quantitative apoptosis-inducing activities of compound **6c** were assessed by flow cytometry using fluorescein isothiocyanate annexin V/propidium iodide (PI) double staining assay. The percentage of apoptotic cells (annexin V^+/PI^- staining) in the control group was 5.9% (Fig. 5A). After treatment with 2 μM, 4 μM and 8 μM of compound **6c** for 24 h, the percentages of apoptotic cells (lower right section of fluorocytogram) increased to 9.1% (Fig. 5B), 18.3% (Fig. 5C) and 22.2% (Fig. 5D), respectively. All the evidence revealed compound **6c** as a potent apoptosis inducer in the human lung cancer cell line in a dose-dependent manner, the anti-proliferative activity of which was associated with apoptosis rather than with a toxic effect.

Furthermore, the contribution of compound **6c** to cell cycle progression was evaluated. Synchronized A549 cells were treated with 2 μM, 4 μM and 8 μM of compound **6c** for 24 h and then subjected to flow cytometric analysis after DNA staining with PI. The results of cell cycle distribution were illustrated in Fig. 6. It was demonstrated that the exposure of A549 cells to gradient concentrations of compound **6c** led to a significant decrease of cell population in S phase accompanied by a slight increase in G1 phase in comparison to the control group. These results suggested that the anti-proliferative activity and apoptosis-inducing effect of compound **6c** were correlated with a substantial cell cycle arrest at S phase in A549 cells.

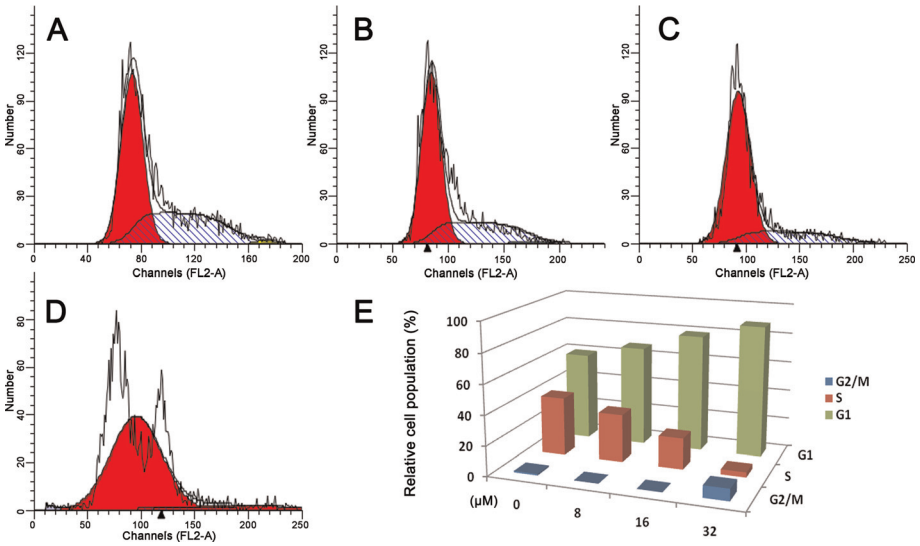

Fig. 6 Effect of **11a** on cell cycle progression on A549 cells. (A) Control group; (B) 2 μM of **6c**; (C) 4 μM of **6c**; (D) 8 μM of **6c**; (E) quantitative cell cycle distribution of **6c**.

Conclusions

We present herein a regioselective chemical strategy that allows the synthesis of novel aza-caged *Garcinia* analogues with the 4-aza-tricyclo[4.3.1.$0^{3,7}$] dec-2-one scaffold and their biological evaluation. Actually, this aza-caged scaffold provides a suitable site for chemical modification that will help further understanding of the SAR around the caged region and improving the activity and drug-like properties. In the study of Clasien/Diels–Alder reaction, we observed that precursor **7** containing an intramolecular hydrogen bond produces an unexpected allyl migration product. We have also discovered that precursors **20a–e** with a C–N bond at the C5 position perform a regioselective Claisen/Diels–Alder cascade reaction while corresponding precursor **25** with a C–O bond is not regioselective. These phenomena are explained according to the DFT energy calculation. We have also described the preliminary SAR by their anti-proliferative and IKKβ inhibitory activity and further illustrated the binding mode of IKKβ with the analogues by molecular docking simulation. The results suggest that introduction of hydrophobic moiety to the caged region improves the cytotoxicity and IKKβ inhibition. The aza-caged compound **6c** has been shown to induce apoptosis and cell cycle S phase arrest in A549 cells. These findings enhance our understanding of the SAR and help the discovery of the novel aza-caged *Garinia* xanthones as potential anti-tumor agents.

Experimental

General notes

All reagents were purchased from commercial sources and were used without further purification unless otherwise noted. Microwave irradiation was carried out with a single mode cavity Discover microwave synthesizer (CEM Corp., NC). Organic solutions were concentrated by rotary evaporator (Büchi Rotavapor) below 45 °C under reduced pressure. Reactions were monitored by thin-layer chromatography (TLC) carried out on 0.25 mm silica gel plates (GF254) and visualized under UV light. Silica gel (60 Å, 300–400 mesh) was used for flash column chromatography. Melting points were determined with a Melt-Temp II apparatus and were reported without any correction. IR spectra were recorded on a Nicolet iS10 Avatar FT-IR spectrometer using KBr film. The ^{1}H NMR and ^{13}C NMR spectra were collected on Bruker AV-300 and/or Bruker AV-500 instruments using deuterated solvents with tetramethylsilane (TMS) as internal standard. The multiplicity was defined by a s (singlet), d (doublet), t (triplet) or m (multiplet). EI-MS was recorded on Shimadzu GCMS-2010 apparatus. High resolution mass spectra (HRMS) were recorded on a Water Q-Tof micro.

GA was isolated and purified according to the previously reported methods.[26] The cluvenone was synthesized according to the previously reported methods. [15] The purity of GA used in all experiments was 95% or higher. It was dissolved in PBS containing arginine to a concentration of 10 mM as the primary stock solution and stored at −20 °C. 3-(4,5-Dimethylthiazol-2-yl)-2,5-diphenyltetrazoliumbromide (MTT) was purchased from Sigma (St Louis, MO). Annexin V-FITC Apoptosis Detection kit was purchased from BioVision (Mountain View, CA). HTScan IKKβ kinase assay kit was purchased from Cell Signaling Technology (Beverly, MA). Human IκBα and p-IκBα (Ser 32/36) antibodies were bought from Santa Cruz Biotechnology, Inc. (Santa Cruz, CA). All drugs were diluted in the corresponding culture medium to desired concentrations before use.

Human hepatocellular carcinoma HepG2 cell line, human lung carcinoma A549 cell line and human glioblastoma U251 cell line were purchased from Cell Bank of Shanghai Institute of Biochemistry and Cell Biology, Shanghai Institutes for Biological Sciences, Chinese Academy of Sciences. HepG2, A549 and U251 cells were cultured in DMEM which were supplemented with 10% (v/v) fetal calf serum, 100 U mL^{-1} penicillin and 100 U mL^{-1} streptomycin in a 5% CO_2 atmosphere.

(2,4-Dihydroxyphenyl)(2-hydroxyphenyl)methanone (11)

$POCl_3$ (60 mL) followed by anhydrous $ZnCl_2$ (21.76 g, 160 mmol) was added to a round-bottomed flask containing salicylic acid (**9**) (5.52 g, 40 mmol) and resorcinol (**10**) (5.28 g, 48 mmol). The reaction vessel was then equipped with a reflux condenser and stirred under nitrogen at 68 °C for 2 h. The red colored reaction mixture was then cooled to 25 °C and poured into a beaker of about 1000 g of ice. The precipitate was filtered, washed with ice brine (200 mL × 3) and dried. The crude material was purified by flash column chromatography (30% EtOAc–PE) to yield benzophenone **11** (6.62 g, 72%) as a yellow solid. mp: 131–132 °C; R_f = 0.58 (20% EtOAc–hexane); ^{1}H NMR (300 MHz, DMSO-d_6): δ 12.45 (s, 1H), 10.72 (s, 1H), 10.09 (s, 1H), 7.40–7.35 (m, 1H), 7.27–7.21 (m, 2H), 7.01–6.90 (m, 2H), 6.46–6.28 (m, 2H); ^{13}C NMR (75 MHz, DMSO-d_6): δ 199.95, 164.92, 164.23, 154.61, 135.64, 131.71, 128.86, 125.67, 118.85, 116.21, 113.33, 108.16, 102.27; IR (KBr, cm^{-1}): 3384, 3196, 3090, 1629, 1580, 1486, 1281, 1234, 1159, 755; EI-MS (*m*/*z*): 230 (M^+) (24); HRMS (ESI) calc. for $C_{13}H_{10}O_4$ $(M - H)^-$ 229.0501, found 229.0504.

3-Hydroxy-9*H*-xanthen-9-one (12)

A sealed glass tube containing a suspension of benzophenone **11** (690 mg, 3 mmol) and sodium acetate (24.6 mg, 0.3 mmol) in water (5 mL) was introduced into the cavity of CEM microwave reactor and irradiated at 150 W, 120 °C for 8 min under magnetic stirring. After cooling to 25 °C by an air-flow, the tube was removed from the rotor. The reaction mixture was diluted with ice water (5 mL). The precipitate was filtered, washed with ice water (5 mL × 3) and dried to yield xanthone **12** (630 mg, 99%) as a white solid. mp: 254–255 °C; R_f = 0.32 (20% EtOAc–hexane); ^{1}H NMR (300 MHz, DMSO-d_6): δ 11.02 (br, 1H), 8.15 (d, J = 7.8 Hz, 1H), 8.05 (d, J = 8.7 Hz, 1H), 7.82 (t, J = 7.8 Hz, 1H), 7.60 (d, J = 8.4 Hz, 1H), 7.44 (t, J = 7.5 Hz, 1H), 6.94–6.89 (m, 2H); ^{13}C NMR (125 MHz, DMSO-d_6): δ 174.73, 164.00, 157.54, 155.54, 134.74, 129.97, 125.82, 124.07, 121.20, 117.83, 114.11, 113.99, 102.12; IR (KBr, cm^{-1}): 3137, 1614, 1561, 1455, 1310, 844, 751; EI-MS (*m*/*z*): 212 (M^+) (100); HRMS (ESI) calc. for $C_{13}H_8O_3$ $(M - H)^-$ 211.0395, found 211.0400.

3-Hydroxy-4-nitro-9*H*-xanthen-9-one (13)

50% nitric acid (5.1 mL, 40 mmol) was added to a suspension of xanthone **12** (4.24 g, 20 mmol) in acetic acid (100 mL) at 25 °C. The reaction mixture was stirred under nitrogen at 60 °C for 30 min and the reaction suspension was turned into a red solution. The solution was stirred at 60 °C for next 20 min and a yellow precipitate was formed. The reaction mixture was then cooled to 25 °C and poured into ice water (500 mL). The precipitate was filtered, washed with ice water (100 mL × 3) and dried. The crude material was purified by flash column chromatography (60% CH_2Cl_2–PE) to yield compound **13** (2.98 g, 58%) as a pale-yellow solid. mp: 220–222 °C; R_f = 0.60 (50% EtOAc–hexane); ^{1}H NMR (300 MHz, DMSO-d_6): δ 12.63 (br, 1H), 8.17 (d, J = 9.0 Hz, 1H), 8.14–8.11 (m, 1H), 7.83–7.79 (m, 1H), 7.59–7.55 (m, 1H), 7.49–7.44 (m, 1H), 7.12 (d, J = 9.0 Hz, 1H); ^{13}C NMR (75 MHz, DMSO-d_6): δ 173.76, 155.54, 154.82, 148.36, 135.42, 129.27, 128.25, 125.93, 125.13, 121.01, 117.91, 114.04, 113.61; IR (KBr, cm^{-1}): 3085, 1614, 1534, 1449, 1322, 765; EI-MS (*m*/*z*): 257 (M^+) (100); HRMS (ESI) calc. for $C_{13}H_7NO_5$ $(M - H)^-$ 256.0246, found 211.0250.

4-Amino-3-hydroxy-9*H*-xanthen-9-one (8)

Pd/C (250 mg) was added to a solution of compound **13** (2.57 g, 10 mmol) in THF (25 mL) and methanol (25 mL). The reaction mixture was degassed using nitrogen and stirred under an atmosphere of hydrogen for 3 h at 25 °C, and then filtered through a plug of silica gel. The filtration was concentrated and dried to yield compound **8** (2.23 g, 98%) as a yellow solid. mp: 241–243 °C; R_f = 0.33 (50% EtOAc–hexane); ^{1}H NMR (300 MHz, DMSO-d_6): δ 10.56 (br, 1H), 8.20 (d, J = 6.9 Hz, 1H), 7.98–7.81 (m, 1H), 7.72 (d, J = 7.8 Hz, 1H), 7.48–7.41 (m, 2H), 6.94 (d, J = 8.1 Hz, 1H), 5.06 (br, 2H); ^{13}C NMR (75 MHz, DMSO-d_6): δ 175.53, 155.52, 148.98, 144.33, 134.50, 125.84, 124.12, 123.69, 120.78, 117.96, 114.53, 113.18, 112.15; IR (KBr, cm^{-1}): 3404, 3316, 3198, 1591, 1563, 1453, 1345, 1054; EI-MS (*m*/*z*): 227 (M^+) (100); HRMS (ESI) calc. for $C_{13}H_9NO_3$ $(M + H)^+$ 228.0661, found 228.0665.

4-(Allylamino)-3-(allyloxy)-9*H*-xanthen-9-one (7), 3-(allyloxy)-4-amino-9*H*-xanthen-9-one (14), and 3-(allyloxy)-4-(diallylamino)-9*H*-xanthen-9-one (20b)

Potassium carbonate (1.518 g, 11 mmol) was added to a solution of compound **8** (1.135 g, 5 mmol) in dried acetone (20 mL). The reaction vessel was then equipped with a reflux condenser, and the mixture was stirred under nitrogen at 45 °C for 20 min. A solution of allyl chloride (760 mg, 10 mmol) in dried acetone (10 mL) was then added to the stirring reaction mixture dropwise over 1 h and the mixture was further stirred at 45 °C for another 1 h. The reaction mixture was allowed to cool to 25 °C and then partitioned between EtOAc (30 mL) and water (70 mL). The water layer was back-extracted with EtOAc (30 mL × 2) and the combined organic layers were dried over $MgSO_4$, filtered and concentrated. The residue was purified by flash column chromatography (10–20% EtOAc–PE) to yield compound **7** (584 mg, 38%) as a yellow solid, compound **14** (601 mg, 45%) as a yellow solid, and compound **20b** (174 mg, 10%) as a yellow solid, respectively. Compound **7**: mp: 114–116 °C; R_f = 0.48 (20% EtOAc–hexane); ^{1}H NMR (300 MHz, $CDCl_3$): δ 8.32 (d, J = 7.8 Hz, 1H), 7.87 (d, J = 9.0 Hz, 1H), 7.70 (t, J = 7.5 Hz, 1H), 7.52 (d, J = 8.4 Hz, 1H), 7.36 (t, J = 7.5 Hz, 1H), 6.94 (d, J = 9.0 Hz, 1H), 6.15–5.95 (m, 2H), 5.45 (d, J = 17.1 Hz, 1H), 5.35 (d, J = 10.5 Hz, 1H), 5.30 (s, 1H), 5.24 (d, J = 17.1 Hz, 1H), 5.10 (d, J = 10.2 Hz, 1H), 4.72 (d, J = 5.1 Hz, 2H), 4.13 (d, J = 5.7 Hz, 2H); ^{13}C NMR (75 MHz, $CDCl_3$): δ 176.93, 155.99, 153.03, 147.88, 136.58, 134.33, 132.51, 126.73, 125.91, 123.76, 121.48, 118.39, 118.28, 117.80, 116.78, 116.09, 108.99, 69.89, 49.83; IR (KBr, cm^{-1}): 3410, 3080, 2855, 1656, 1602, 1467, 1440, 1428, 1347, 1227, 1090, 758; EI-MS (*m*/*z*): 307 (M^+) (100); HRMS (ESI) calc. for $C_{19}H_{17}NO_3$ $(M + H)^+$ 308.1287, found 308.1292. Compound **14**: mp: 121–122 °C; R_f = 0.38 (20% EtOAc–hexane); ^{1}H NMR (300 MHz, $CDCl_3$): δ

8.34 (d, J = 8.1 Hz, 1H), 7.74 (d, J = 9.0 Hz, 1H), 7.68 (d, J = 7.8 Hz, 1H), 7.50 (d, J = 8.4 Hz, 1H), 7.36 (d, J = 7.5 Hz, 1H), 6.93 (d, J = 8.1 Hz, 1H), 6.15–6.07 (m, 1H), 5.46 (d, J = 17.4 Hz, 1H), 5.35 (d, J = 10.5 Hz, 1H), 4.73 (d, J = 1.8 Hz, 2H), 4.20 (br, 2H); ^{13}C NMR (75 MHz, $CDCl_3$): δ 176.42, 155.54, 149.26, 144.35, 133.75, 132.14, 126.34, 123.92, 123.21, 121.12, 117.86, 117.14, 115.86, 114.98, 108.05, 69.19; IR (KBr, cm^{-1}): 3432, 3339, 3086, 3020, 2926, 1665, 1605, 1486, 1450, 1345, 1295, 906, 755; EI-MS (m/z): 267 (M^+) (23); HRMS (ESI) calc. for $C_{16}H_{13}NO_3$ $(M + H)^+$ 268.0974, found 268.00978. Compound **20b**: mp: 105–107 °C; R_f = 0.63 (20% EtOAc–hexane); ^{1}H NMR (300 MHz, $CDCl_3$): δ 8.31 (d, J = 7.8 Hz, 1H), 8.10 (dd, J = 9.0, 0.9 Hz, 1H), 7.72 (t, J = 8.4 Hz, 1H), 7.54 (d, J = 8.4 Hz, 1H), 7.35 (t, J = 7.5 Hz, 1H), 6.93 (d, J = 8.4 Hz, 1H), 6.10–6.05 (m, 1H), 5.94–5.83 (m, 2H), 5.48 (d, J = 17.1 Hz, 1H), 5.33 (d, J = 10.5 Hz, 1H), 5.17 (d, J = 17.1 Hz, 2H), 4.98 (d, J = 9.9 Hz, 2H), 4.69 (d, J = 0.9 Hz, 2H), 3.87 (s, 2H), 3.85 (s, 2H); ^{13}C NMR (75 MHz, $CDCl_3$): δ 176.91, 161.24, 156.21, 154.92, 136.38 (2C), 134.29, 132.63, 126.56, 126.51, 123.70, 121.54, 117.98, 117.86, 116.64, 116.25, 109.48, 69.47, 55.92; IR (KBr, cm^{-1}): 3061, 2908, 2867, 1658, 1613, 1598, 1467, 1432, 1276, 1107, 1086, 917, 764, 751; EI-MS (m/z): 347 (M^+) (36); HRMS (ESI) calc. for $C_{22}H_{21}NO_3$ $(M + H)^+$ 348.1600, found 348.1606.

4-(Diallylamino)-3-hydroxy-9*H*-xanthen-9-one (17)

A solution of **7** (80 mg, 0.3 mmol) in decalin was stirred under nitrogen at 180 °C for 3 h. The yellow reaction mixture was then cooled to 25 °C and the residue was purified by flash column chromatography (5–10% EtOAc–PE) to yield compound **17** (46.5 mg, 58%) as a yellow solid. mp: 109–111 °C; R_f = 0.48 (20% EtOAc–hexane); ^{1}H NMR (300 MHz, $CDCl_3$): δ 8.34 (d, J = 7.8 Hz, 1H), 8.22 (d, J = 5.1 Hz, 1H), 7.32 (t, J = 7.5 Hz, 1H), 7.52 (d, J = 8.4 Hz, 1H), 7.41 (t, J = 7.5 Hz, 1H), 6.99 (d, J = 8.7 Hz, 1H), 5.88–5.76 (m, 2H), 5.15 (s, 1H), 5.10–5.04 (m, 4H), 3.90–3.69 (m, 4H); ^{13}C NMR (75 MHz, $CDCl_3$): δ 175.83, 160.08, 155.04, 155.01, 133.84, 133.77, 126.36, 126.04, 123.70, 121.33, 121.15, 118.30, 117.05, 115.09, 110.85, 56.72; IR (KBr, cm^{-1}): 3286, 3067, 2926, 1649, 1601, 1464, 1440, 1325, 1225, 754; EI-MS (m/z): 307 (M^+) (59); HRMS (ESI) calc. for $C_{19}H_{17}NO_3$ $(M + H)^+$ 308.1287, found 308.1292.

General procedure for the synthesis of compounds 20a–e

Potassium carbonate (276 g, 0.2 mmol) was added to a solution of compound **7** (307 mg, 0.1) in dried acetone at 25 °C followed by the corresponding halide (0.15 mmol). The reaction mixture was stirred overnight at 25 °C and filtered. The filtration was concentrated and the residue was purified by flash column chromatography (10% EtOAc–PE) to yield compounds **20a–e**, respectively.

4-(Allyl(methyl)amino)-3-(allyloxy)-9*H*-xanthen-9-one (20a)

Compound **20a** (318 mg, 99%) was prepared from compound **7** and methyl iodide as a yellow solid. mp: 110–112 °C; R_f = 0.55 (20% EtOAc–hexane); ^{1}H NMR (300 MHz, $CDCl_3$): δ 8.32 (dd, J = 7.8, 1.5 Hz, 1H), 8.09 (d, J = 9.0 Hz, 1H), 7.71 (dt, J = 8.4, 1.5 Hz, 1H), 7.54 (d, J = 8.4 Hz, 1H), 7.36 (t, J = 7.5 Hz, 1H), 6.95 (d, J = 9.0 Hz, 1H), 6.16–6.02 (m, 1H), 5.99–5.89 (m, 1H), 5.47 (dd, J = 17.4, 1.5 Hz, 1H), 5.34 (dd, J = 10.5, 1.2 Hz, 1H), 5.19 (d, J = 17.1 Hz, 1H), 5.06 (d, J = 9.9 Hz, 1H), 4.71 (d, J = 5.1 Hz, 2H), 3.83 (d, J = 6.3 Hz, 2H), 2.09 (s, 3H); ^{13}C NMR (75 MHz, $CDCl_3$): δ 176.97, 160.71, 156.23, 154.51, 136.34, 134.28, 132.68, 128.29, 126.58, 123.72, 123.31, 121.52, 118.05, 117.99, 116.81, 116.42, 109.82, 69.65, 58.63, 40.76; IR (KBr, cm^{-1}): 3097, 2926, 2861, 1661, 1602, 1467, 1441, 1332, 1287, 1227, 1082, 768, 748; EI-MS (m/z): 321 (M^+) (13); HRMS (ESI) calc. for $C_{20}H_{19}NO_3$ $(M + H)^+$ 322.1443, found 322.1437.

4-(Allyl(benzyl)amino)-3-(allyloxy)-9*H*-xanthen-9-one (20c)

Compound **20c** (395 mg, 99%) was prepared from compound **7** and benzyl bromide as a yellow solid. mp: 78–80 °C; R_f = 0.63 (20% EtOAc–hexane); ^{1}H NMR (300 MHz, $CDCl_3$): δ 8.31 (dd, J = 7.8, 1.5 Hz, 1H), 8.08 (d, J = 9.0 Hz, 1H), 7.70 (dt, J = 7.8, 1.5 Hz, 1H), 7.51 (d, J = 8.1 Hz, 1H), 7.43 (d, J = 7.2 Hz, 2H), 7.34 (t, J = 7.5 Hz, 1H), 7.23 (t, J = 7.2 Hz, 2H), 7.18–7.13 (m, 1H), 6.90 (d, J = 9.0 Hz, 1H), 6.13–6.02 (m, 1H), 6.96–5.85 (m, 1H), 5.48 (dd, J = 17.4, 1.5 Hz, 1H), 5.34 (dd, J = 10.8, 1.5 Hz, 1H), 5.13 (dd, J = 17.1, 1.5 Hz, 1H), 4.98 (d, J = 10.2 Hz, 1H), 4.66 (d, J = 5.1 Hz, 2H), 4.40 (s, 2H), 3.83 (d, J = 6.3 Hz, 2H); ^{13}C NMR (75 MHz, $CDCl_3$): δ 177.00, 161.46, 156.23, 155.00, 139.90, 136.23, 134.33, 132.63, 130.91, 128.85, 128.43, 127.97, 126.77, 126.60, 123.93, 123.72, 121.53, 117.94, 116.63, 116.43, 109.39, 69.49, 57.22, 55.71; IR (KBr, cm^{-1}): 3068, 3032, 2926, 2849, 1658, 1614, 1598, 1466, 1432, 1277, 1219, 1104, 918, 752; EI-MS (m/z): 397 (M^+) (7); HRMS (ESI) calc. for $C_{26}H_{23}NO_3$ $(M + H)^+$ 398.1756, found 398.1764.

4-(Allyl(4-fluorobenzyl)amino)-3-(allyloxy)-9*H*-xanthen-9-one (20d)

Compound **20d** (408 mg, 98%) was prepared from compound **7** and 4-fluorobenzyl bromide as a yellow solid. mp: 84–86 °C; R_f = 0.64 (20% EtOAc–hexane); ^{1}H NMR (300 MHz, $CDCl_3$): δ 8.31 (d, J = 7.8 Hz, 1H), 8.08 (d, J = 9.0 Hz, 1H), 7.74–7.69 (m, 1H), 7.51 (d, J = 7.8 Hz, 1H), 7.40–7.34 (m, 3H), 6.94–6.88 (m, 3H), 6.14–6.03 (m, 1H), 5.95–5.86 (m, 1H), 5.48 (d, J = 17.1 Hz, 1H), 5.36 (d, J = 10.5 Hz, 1H), 5.12 (d, J = 16.8 Hz, 1H), 4.98 (d, J = 10.2 Hz, 1H), 4.68 (d, J = 5.1 Hz, 2H), 4.36 (s, 2H), 3.80 (d, J = 6.3 Hz, 2H); ^{13}C NMR (75 MHz, $CDCl_3$): δ 176.88, 161.87 ($^1J_{CF}$ = 240.2 Hz), 161.43, 156.18, 154.97, 136.11, 135.52, 134.37, 132.55, 129.87 ($^3J_{CF}$ = 7.5 Hz), 126.66, 126.49, 124.11, 123.79, 121.55, 118.01, 117.84, 116.64, 116.54, 114.72 ($^2J_{CF}$ = 21.0 Hz), 109.32, 69.48, 56.40, 55.76; IR (KBr, cm^{-1}): 3085, 2932, 2844, 1657, 1599, 1508, 1466, 1433, 1223, 775, 760, 734; EI-MS (m/z): 415 (M^+) (17); HRMS (ESI) calc. for $C_{26}H_{22}FNO_3$ $(M + H)^+$ 416.1662, found 416.1656.

4-(Allyl(4-chlorobenzyl)amino)-3-(allyloxy)-9*H*-xanthen-9-one (20e)

Compound **20e** (424 mg, 98%) was prepared from compound **7** and 4-chlorobenzyl bromide as a yellow solid. mp: 83–84 °C; R_f

= 0.64 (20% EtOAc–hexane); ^{1}H NMR (300 MHz, $CDCl_3$): δ 8.32 (dd, J = 8.4, 1.5 Hz, 1H), 8.10 (d, J = 9.0 Hz, 1H), 7.72 (dt, J = 8.7, 1.5 Hz, 1H), 7.51 (d, J = 8.4 Hz, 1H), 7.40–7.36 (m, 3H), 7.20 (d, J = 8.4 Hz, 2H), 6.92 (d, J = 9.0 Hz, 1H), 6.17–6.04 (m, 1H), 5.97–5.84 (m, 1H), 5.49 (dd, J = 17.1, 1.2 Hz, 1H), 5.37 (dd, J = 10.5, 0.9 Hz, 1H), 5.11 (d, J = 17.1 Hz, 1H), 4.98 (d, J = 9.9 Hz, 1H), 4.68 (d, J = 5.1 Hz, 2H), 4.37 (s, 2H), 3.80 (d, J = 6.0 Hz, 2H); ^{13}C NMR (75 MHz, $CDCl_3$): δ 176.87, 161.36, 156.17, 154.91, 138.51, 136.00, 134.41, 132.52, 132.40, 129.71, 128.13, 126.67, 126.46, 124.16, 123.83, 121.55, 118.07, 117.84, 116.66, 116.64, 109.33, 69.49, 56.48, 55.84; IR (KBr, cm^{-1}): 3068, 2926, 2855, 1658, 1598, 1466, 1432, 1277, 765, 752; EI-MS (m/z): 431 (M^+) (9); HRMS (ESI) calc. for $C_{26}H_{22}ClNO_3$ $(M + H)^+$ 432.1366, found 432.1371.

General procedure for the synthesis of compounds 6a–e

A solution of **20a–e** (0.15 mmol) in decalin was stirred under nitrogen at 180 °C for 3 h. The yellow reaction mixture was then cooled to 25 °C and the residue was purified by flash column chromatography (5–10% EtOAc–PE) to yield aza-caged compounds **6a–e**, respectively.

Aza-caged compound (6a)

Compound **6a** (25.6 mg, 53%) was prepared from compound **20a** (48.2 mg, 0.15 mmol) as a yellow solid. mp: 126–128 °C; R_f = 0.48 (20% EtOAc–hexane); ^{1}H NMR (300 MHz, $CDCl_3$): δ 7.93 (dd, J = 7.8, 1.5 Hz, 1H), 7.53 (dt, J = 6.9, 1.5 Hz, 1H), 7.31 (d, J = 6.9 Hz, 1H), 7.11–7.03 (m, 2H), 5.29–5.18 (m, 1H), 4.66 (d, J = 10.2 Hz, 1H), 4.51 (d, J = 16.5 Hz, 1H), 3.90–3.83 (m, 1H), 3.41 (dd, J = 6.6, 2.4 Hz, 1H), 2.72–2.67 (m, 2H), 2.47 (s, 3H), 2.41–2.33 (m, 2H), 1.75–1.71 (m, 2H); ^{13}C NMR (75 MHz, $CDCl_3$): δ 200.55, 177.18, 160.05, 136.36, 136.12, 132.99, 132.69, 127.21, 121.82, 119.52, 118.73, 118.12, 89.85, 70.72, 60.52, 46.46, 39.26, 36.23, 33.01, 30.69; IR (KBr, cm^{-1}): 3079, 2920, 2843, 1771, 1722, 1671, 1642, 1609, 1464, 1315, 1275, 1261,764; EI-MS (m/z): 321 (M^+) (52); HRMS (ESI) calc. for $C_{20}H_{19}NO_3$ $(M + H)^+$ 322.1443, found 322.1436.

Aza-caged compound (6b)

Compound **6b** (33.8 mg, 65%) was prepared from compound **20b** (52.1 mg, 0.15 mmol) as a yellow solid. mp: 113–114 °C; R_f = 0.54 (20% EtOAc–hexane); ^{1}H NMR (300 MHz, $CDCl_3$): δ 7.93 (dd, J = 7.8, 1.5 Hz, 1H), 7.53 (dt, J = 6.9, 1.5 Hz, 1H), 7.30 (d, J = 6.9 Hz, 1H), 7.08–7.02 (m, 2H), 5.88–5.79 (m, 1H), 5.29–5.21 (m, 2H), 5.11 (d, J = 10.2 Hz, 1H), 4.64 (d, J = 9.9 Hz, 1H), 4.49 (d, J = 16.8 Hz, 1H), 3.73 (dd, J = 9.6, 4.5 Hz, 1H), 3.53 (dd, J = 7.8, 1.5 Hz, 1H), 3.43–3.38 (m, 1H), 3.05 (dd, J = 14.7, 6.6 Hz, 1H), 2.71–2.64 (m, 2H), 2.44–2.40 (m, 1H), 2.37–2.31 (m, 1H), 1.73–1.70 (m, 2H); ^{13}C NMR (75 MHz, $CDCl_3$): δ 201.04, 177.20, 160.12, 136.53, 136.26, 136.10, 132.88, 132.75, 127.17, 121.71, 119.53, 118.48, 118.10, 116.27, 89.84, 70.19, 57.77, 52.05, 46.36, 39.23, 33.31, 30.27; IR (KBr, cm^{-1}): 3062, 2927, 2850, 1731, 1676, 1642, 1608, 1464, 1269, 1260, 758, 744; EI-MS (m/z): 347 (M^+) (15); HRMS (ESI) calc. for $C_{22}H_{21}NO_3$ $(M + H)^+$ 348.1600, found 348.1608.

Aza-caged compound (6c)

Compound **6c** (28.6 mg, 48%) was prepared from compound **20c** (59.6 mg, 0.15 mmol) as a yellow solid. mp: 107–108 °C; R_f = 0.55 (20% EtOAc–hexane); ^{1}H NMR (300 MHz, $CDCl_3$): δ 7.95 (dd, J = 7.8, 1.5 Hz, 1H), 7.55 (dt, J = 6.9, 1.5 Hz, 1H), 7.37–7.33 (m, 5H), 7.29 (m, 1H), 7.12–7.04 (m, 2H), 5.36–5.29 (m, 1H), 4.67 (d, J = 10.2 Hz, 1H), 4.52 (d, J = 17.1 Hz, 1H), 4.15 (d, J = 14.4 Hz, 1H), 3.68 (dd, J = 9.3, 4.5 Hz, 1H), 3.58 (d, J = 14.4 Hz, 1H), 3.48–3.45 (m, 1H), 2.74 (dd, J = 13.5, 5.1 Hz, 1H), 2.58–2.49 (m, 2H), 2.38–2.32 (m, 1H), 1.76–1.73 (m, 2H); ^{13}C NMR (75 MHz, $CDCl_3$): δ 201.26, 177.28, 160.19, 139.80, 136.35, 136.09, 133.03, 132.68, 128.38, 127.99, 127.24, 126.94, 121.78, 119.54, 118.65, 118.14, 89.81, 70.38, 58.20, 53.20, 46.44, 39.23, 33.49, 30.50; IR (KBr, cm^{-1}): 3086, 2924, 2853, 1772, 1645, 1611, 1460, 1275, 1260, 762, 752; EI-MS (m/z): 397 (M^+) (8); HRMS (ESI) calc. for $C_{26}H_{23}NO_3$ $(M + H)^+$ 398.1756, found 398.1765.

Aza-caged compound (6d)

Compound **6d** (28.7 mg, 46%) was prepared from compound **20d** (62.4 mg, 0.15 mmol) as a yellow solid. mp: 111–112 °C; R_f = 0.56 (20% EtOAc–hexane); ^{1}H NMR (300 MHz, $CDCl_3$): δ 7.95 (d, J = 7.5, 1H), 7.55 (t, J = 7.5, 1H), 7.33–7.31 (m, 3H), 7.11–7.00 (m, 4H), 5.38–5.29 (m, 1H), 4.68 (d, J = 9.9 Hz, 1H), 4.53 (d, J = 17.1 Hz, 1H), 4.10 (d, J = 14.4 Hz, 1H), 3.70–3.61 (m, 1H), 3.56 (d, J = 14.4 Hz, 1H), 3.47–3.45 (m, 1H), 2.76–2.70 (m, 1H), 2.56–2.53 (m, 2H), 2.37–2.35 (m, 1H), 1.74–1.72 (m, 2H); ^{13}C NMR (75 MHz, $CDCl_3$): δ 201.16, 177.19, 163.42 ($^1J_{CF}$ = 243.8 Hz), 160.07, 136.35, 136.02, 134.81, 132.97, 132.50, 129.47 ($^3J_{CF}$ = 8.9 Hz), 127.25, 121.83, 119.56, 118.74, 118.10, 115.18 ($^2J_{CF}$ = 21.1 Hz), 89.79, 70.39, 58.16, 52.58, 46.41, 39.18, 33.46, 30.52; IR (KBr, cm^{-1}): 3088, 2962, 2852, 1776, 1635, 1465, 1266, 1213, 764; EI-MS (m/z): 415 (M^+) (14); HRMS (ESI) calc. for $C_{26}H_{22}FNO_3$ $(M + H)^+$ 416.1662, found 416.1655.

Aza-caged compound (6e)

Compound **6e** (29.7 mg, 46%) was prepared from compound **20e** (64.6 mg, 0.15 mmol) as a yellow solid. mp: 110–112 °C; R_f = 0.56 (20% EtOAc–hexane); ^{1}H NMR (300 MHz, $CDCl_3$): δ 7.95 (d, J = 7.8, 1H), 7.55 (t, J = 6.9, 1H), 7.35–7.33 (m, 1H), 7.33–7.28 (m, 4H), 7.10–7.04 (m, 2H), 5.36–5.24 (m, 1H), 4.67 (d, J = 10.2 Hz, 1H), 4.52 (d, J = 16.8 Hz, 1H), 4.14 (d, J = 14.7 Hz, 1H), 3.65 (dd, J = 9.3, 4.5 Hz, 1H), 3.54 (d, J = 14.4 Hz, 1H), 3.46–3.44 (m, 1H), 2.69–2.65 (m, 1H), 2.54–2.50 (m, 2H), 2.37–2.35 (m, 1H), 1.75–1.72 (m, 2H); ^{13}C NMR (75 MHz, $CDCl_3$): δ 201.19, 177.17, 160.08, 138.22, 136.36, 136.03, 132.96, 132.65, 132.46, 129.32, 128.54, 127.26, 121.85, 119.55, 118.77, 118.09, 89.75, 70.35, 58.24, 52.66, 46.38, 39.20, 33.49, 30.52; IR (KBr, cm^{-1}): 3080, 2924, 2861, 1764, 1644, 1608, 1464, 1257, 1225, 763; EI-MS (m/z): 431 (M^+)

(12); HRMS (ESI) calc. for $C_{26}H_{22}ClNO_3$ $(M + H)^+$ 432.1366, found 432.1372.

MTT assay

Cell viabilities were measured by a colorimetric assay using 3-(4,5-dimethylthiazol-2-yl)-2,5-diphenyltetrazoliumbromide (MTT; Roche, Ltd) as described previously.[27] Experiments were carried out in triplicate in a parallel manner for each concentration of target compounds used and the results were presented as mean ± SE. Control cells were given only culture media. After incubation for 24 h, absorbance (A) was measured at 570 nm. Survival ratio (%) was calculated using the following equation: survival ratio (%) = $(A_{treatment}/A_{control}) \times 100\%$. IC_{50} was taken as the concentration that caused 50% inhibition of cell viabilities and calculated by the SigmaPlot software (Systat Software Inc., USA).

Cell morphological assessment

To detect morphological evidence of apoptosis, cell nuclei were visualized following DNA staining with the fluorescent dye DAPI. Briefly, cells were seeded at a concentration of 1×10^5 cells per well in 6-well tissue culture plates and treated with indicated concentration of **6c**. At the end of incubation, the morphology of cells was monitored under an inverted light microscope. Cells were then fixed with 4% paraform for 20 min and washed with PBS, and then incubated with DAPI (1 μg ml^{-1}) for 10 min. After washing with PBS, cells were observed using fluorescent microscopy (Olympus, Japan) with a peak excitation wave length of 340 nm.

Annexin V/PI double staining assay

Apoptosis-mediated programmed cell death was examined using a double staining method with FITC-labeled annexin V/propidium iodide (PI) apoptosis detection kit (KeyGen, Nanjing, China) according to the manufacturer's instructions. Flow cytometric analysis was performed immediately after supravital staining. Data acquisition and analysis were performed in a Becton Dickinson FACSCalibur flow cytometer using Cell Quest software. Cells in early stages of apoptosis were annexin-V positive; whereas, cells that were both annexin-V and PI positive were in the late stage of apoptosis.

DNA content and cell cycle analyzed by flow cytometry

A549 cells were starved in serum-free medium for 24 h. After treatment with **6c**, cells were collected and fixed in 70% ethanol overnight at 4 °C. Fixed cells were washed with PBS, and resuspended in hypotonic PI staining solution (0.1% (w/v) sodium citrate, 0.1% (v/v) Triton X-100, 0.05 mg ml^{-1} PI, and 0.01 mg ml^{-1} RNase) for 15 min at 37 °C in a dark environment. The stained cells were analyzed using FAScan laser flow cytometry (Becton Dickinson, San Jose, CA).

IKKβ assay

12.5 μL of the 4 × reaction cocktail containing 50 ng IKKβ (supplied from the HTScan IKKβ kinase assay kit, Cell Signaling Technology, Beverly, MA) was incubated with 12.5 μL of test sample for 5 min at room temperature. 25 μL 2× ATP/substrate peptide cocktail was added to the preincubated reaction. After incubation at room temperature for 30 min, a 50 μL stop solution (50 mM EDTA, pH = 8) was added to stop the reaction. Then 25 μL of each reaction were transferred to a 96-well streptavidin-coated plate (PerkinElmer Life Sciences, Boston). After adding 75 μL dH_2O, the mixture was incubated at room temperature for 60 min. After thoroughly washing the wells 3 times with PBST, 100 μL primary antibody [phospho-IκBα (Ser32) (14D4) rabbit mAb, 1 : 1000 in PBS/T with 1% bovine serum albumin (BSA)] was added per well. After 120 min incubation at room temperature, the wells were thoroughly washed 3 times with PBST. 100 μL diluted HRP-labeled anti-rabbit IgG (1 : 1000 in PBS/T with 1% BSA) was added per well. After 30 min incubation at room temperature, the wells were washed five times with PBST. Then 100 μL TMB substrate was added into each well, and the plate was incubated at room temperature for 15 min. After adding the stop solution (100 μL per well), the plate was incubated at room temperature for 15 min and then read at 450 nm with Varioskan spectrofluorometer and spectrophotometer (Thermo, Waltham, MA).

Acknowledgements

Financial support from National Natural Science Foundation of China (No. 90713038, No. 21072231, No. 30873157) and National Major Science and Technology Project of China (Innovation and Development of New Drugs, No. 2008ZX09401–001 and No. 2009ZX09501–003) is acknowledged.

Notes and references

1 (*a*) H. Auterhoff, H. Frauendorf, W. liesenklas and C. Schwandt, *Arch. Pharm.*, 1962, **295**, 833–846; (*b*) W. D. Ollis, B. T. Redman, I. O. Sutherland and K. Jewers, *J. Chem. Soc. D*, 1969, 879–880; (*c*) P. Kumar and P. K. Baslas, *Herba Hungarica*, 1980, **19**, 81–91.
2 (*a*) W. D. Ollis, M. V. J. Ramsy, I. O. Sutherland and S. Mongkolsuk, *Tetrahedron*, 1965, **21**, 1453–1470; (*b*) C. G. Karanjgaonkar, P. M. Nair and K. Venkartaraman, *Tetrahedron Lett.*, 1966, **7**, 687–691; (*c*) J. Asano, K. Chiba, M. Tada and T. Yoshii, *Photochemistry*, 1996, **41**, 815–820; (*d*) Q. B. Han and H. X. Xu, *Curr. Med. Chem.*, 2009, **16**, 3775–3796.
3 (*a*) Q. Guo, Q. Qi, Q. You, H. Gu, L. Zhao and Z. Wu, *Basic Clin. Pharmacol. Toxicol.*, 2001, **31**, 178–184; (*b*) H. Z. Zhang, S. Kasibhatla, Y. Wang, J. Herich, J. Guastella, B. Tseng, J. Drewe and S. X. Cai, *Bioorg. Med. Chem.*, 2004, **12**, 309–317; (*c*) H. Gu, Q. You, W. Liu, Y. Yang, L. Zhao, Q. Qi, J. Zhao, J. Wang, N. Lu, H. Ling, Q. Guo and X. Wang, *Int. Immunopharmacol.*, 2008, **8**, 1493–1502; (*d*) L. Zhao, Q. L. Guo, Q. D. You, Z. Q. Wu and H. Y. Gu, *Drug Chem. Toxicol.*, 2010, **33**, 88–96.
4 T. W. Zhou, *Chin. J. New Drugs*, 2007, **16**, 79–82.
5 (*a*) L. Zhao, Q. L. Guo, Q. D. You, Z. Q. Wu and H. Y. Gu, *Biol. Pharm. Bull.*, 2004, **27**, 998–1003; (*b*) F. Nie, X. Zhang, Q. Qi, L. Yang, Y. Yang, W. Liu, N. Lu, Z. Wu, Q. You and Q. Guo, *Toxicology*, 2009, **260**, 60–67; (*c*) J. J. Rong, R. Hu, Q. Qi, H. Y. Gu, Q. Zhao, J. Wang, R. Mu, Q. D. You and Q. L. Guo, *Cancer Lett.*, 2009, **284**, 102–112; (*d*) H. Huang, D. Chen, S. Li, X. Li, N. Liu, X. Lu, S. Liu, K. Zhao, H. Guo, C. Yang, P. Zhou, X. Dong, C. Zhang, Guanmei, Q. P. Dou and J. Liu, *Cancer Lett.*, 2011, **301**, 221–228.
6 (*a*) J. Yu, Q. L. Guo, Q. D. You, L. Zhao, H. Y. Gu, Y. Yang, H. W. Zhang, Z. Tan and X. Wang, *Carcinogenesis*, 2007, **28**, 632–638;

(*26*) Y. Liu, W. Li, C. Ye, Y. Lin, T. Y. Cheng, M. Wang, H. Zhang, S. Wang, L. Zhang and S. Wang, *J. Atheroscler. Thromb.*, 2010, **17**, 901–913.
7 (*a*) N. Lu, Y. Yang, Q. D. You, Y. Ling, Y. Gao, H. Y. Gu, L. Zhao, X. T. Wang and Q. L. Guo, *Cancer Lett.*, 2007, **258**, 80–89; (*b*) L. Qiang, Y. Yang, Q. D. You, Y. J. Ma, L. Yang, F. F. Nie, H. Y. Hong, L. Zhao, N. Lu, Q. Qi, X. T. Wang and Q. L. Guo, *Biochem. Pharmacol.*, 2008, **75**, 1083–1092; (*c*) T. Li, Z. Yi, S. G. Cho, J. Luo, M. K. Pandey, B. B. Aggarwal and M. Liu, *Cancer Res.*, 2008, **68**, 1843–1850.
8 C. Li, N. Lu, Q. Qi, F. Li, Y. Ling, Y. Chen, Y. Qin, Z. Li, H. Zhang, Q. You and Q. Guo, *Biochem. Pharmacol.*, 2011, **82**, 1873–1883.
9 Y. C. Xin, Q. B. Han, C. Y. Chan, H. Wang, Z. Liu, D. T. Y. Christopher, H. K. Cheng and H. X. Xu, *Proteomics*, 2009, **9**, 242–253.
10 (*a*) L. Zhang, Y. Yi, J. Chen, Y. Sun, Q. Guo, Z. Zheng and S. Song, *Biochem. Biophys. Res. Commun.*, 2010, **403**, 282–287; (*b*) J. Davenport, J. R. Manjarrez, L. Peterson, B. Krumm, B. S. Blagg and R. L. Matts, *J. Nat. Prod.*, 2011, **74**, 1085–1092.
11 M. K. Pandey, B. Sung, K. S. Ahn, A. B. Kunnumakkara, M. M. Chaturvedi and B. B. Aggarwal, *Blood*, 2007, **110**, 3517–3525.
12 S. Kasibhatla, A. Jessen Katayoun, S. Maliartchouk, Y. W. Jean, M. E. Nicole, J. Drewe, L. Qiu, P. A. Shannon, E. P. Anthony, N. Sirisoma, S. Jiang, H. Z. Zhang, R. G. Kurt, X. C. Sui, R. G. Douglas and B. Tseng, *Proc. Natl. Acad. Sci. U. S. A.*, 2005, **102**, 12095–12100.
13 U. D. Palempalli, U. Gandhi, P. Kalantari, H. Vunta, R. J. Arner, V. Narayan, A. Ravindran and K. S. Prabhu, *Biochem. J.*, 2009, **419**, 401–409.
14 Q. Chantarasriwong, W. C. Cho, A. Batowa, W. Chavasiri, C. Moore, A. L. Rheingold and E. A. Theodorakis, *Org. Biomol. Chem.*, 2009, **7**, 4886–4894.
15 X. Wang, N. Lu, Q. Yang, D. Gong, C. Lin, S. Zhang, M. Xi, Y. Gao, L. Wei, Q. Guo and Q. You, *Eur. J. Med. Chem.*, 2011, **46**, 1280–1290.
16 A. Batova, T. Lam, V. Wascholowski, A. L. Yu, A. Giannis and E. A. Theodorakis, *Org. Biomol. Chem.*, 2007, **5**, 494–500.
17 J. Kuemmerle, S. Jiang, B. Tseng, S. Kasibhatla, J. Drewe and S. X. Cai, *Bioorg. Med. Chem.*, 2008, **16**, 4233–4241.
18 For related Claisen/Diels–Alder reaction studies see: (*a*) K. C. Nicolaou and J. Li, *Angew. Chem., Int. Ed.*, 2001, **40**, 4264–4268; (*b*) E. J. Tisdale, I. Slobodov and E. A. Theodorakis, *Org. Biomol. Chem.*, 2003, **1**, 4418–4422; (*c*) E. J. Tisdale, I. Slobodov and E. A. Theodorakis, *Proc. Natl. Acad. Sci. U. S. A.*, 2004, **101**, 12030–12035; (*d*) K. C. Nicolaou, H. Xu and M. Wartmann, *Angew. Chem.*, 2005, **117**, 766–771; (*e*) N. G. Li, J. X. Wang, X. R. Liu, C. J. Lin, Q. D. You and Q. L. Guo, *Tetrahedron Lett.*, 2007, **48**, 6586–6589; (*f*) Z. L. Liu, X. J. Wang, N. G. Li, H. P. Sun, J. X. Wang and Q. D. You, *Tetrahedron*, 2011, **57**, 4774–4779.
19 O. Chantarasriwong, A. Batova, W. Chavasiri and E. A. Theodorakis, *Chem.–Eur. J.*, 2010, **16**, 9944–9962.
20 V. Santagada, F. Frecentese, E. Perissutti, F. Fiorino, B. Severino and G. Caliendo, *Mini-Rev. Med. Chem.*, 2009, **9**, 340–358.
21 N. G. Li, J. X. Wang, Q. D. You, G. Chu and Q. L. Guo, *Chin. J. Chem.*, 2008, **26**, 363–367.
22 M. J. Frisch, G. W. Trucks, H. B. Schlegel, G. E. Scuseria, M. A. Robb, J. R. Cheeseman, J. A. Montgomery, Jr., T. Vreven, K. N. Kudin, J. C. Burant, J. M. Millam, S. S. Iyengar, J. Tomasi, V. Barone, B. Mennucci, M. Cossi, G. Scalmani, N. Rega, G. A. Petersson, H. Nakatsuji, M. Hada, M. Ehara, K. Toyota, R. Fukuda, J. Hasegawa, M. Ishida, T. Nakajima, Y. Honda, O. Kitao, H. Nakai, M. Klene, X. Li, J. E. Knox, H. P. Hratchian, J. B. Cross, V. Bakken, C. Adamo, J. Jaramillo, R. Gomperts, R. E. Stratmann, O. Yazyev, A. J. Austin, R. Cammi, C. Pomelli, J. W. Ochterski, P. Y. Ayala, K. Morokuma, G. A. Voth, P. Salvador, J. J. Dannenberg, V. G. Zakrzewski, S. Dapprich, A. D. Daniels, M. C. Strain, O. Farkas, D. K. Malick, A. D. Rabuck, K. Raghavachari, J. B. Foresman, J. V. Ortiz, Q. Cui, A. G. Baboul, S. Clifford, J. Cioslowski, B. B. Stefanov, G. Liu, A. Liashenko, P. Piskorz, I. Komaromi, R. L. Martin, D. J. Fox, T. Keith, M. A. Al-Laham, C. Y. Peng, A. Nanayakkara, M. Challacombe, P. M. W. Gill, B. Johnson, W. Chen, M. W. Wong, C. Gonzalez and J. A. Pople, *GAUSSIAN 03, revision D.01*, Gaussian, Inc., Wallingford CT, 2004.
23 (*a*) Huheey, A21–A34 (*b*) T. L. Cottrell, *The Strengths of Chemical Bonds*, Butterworths, London, 2nd edn, 1958; (*c*) B. de B. Darwent, *National Standard Reference Data Series*, National Bureau of Standards, Washington, DC, 1970, vol. 31, pp. 1–48; (*d*) S. W. Benson, *J. Chem. Educ.*, 1965, **42**, 502–518.. For the selected bond energies data see the following web page (Visited Date: 2011/12/12): http://www.wiredchemist.com/chemistry/data/bond-energies-lengths
24 G. Xu, Y. Lo, Q. Li, G. Napolitano, X. Wu, X. Jiang, M. Dreano, M. Karin and H. Wu, *Nature*, 2011, **472**, 325–330.
25 (*a*) S. Nagarajan, M. Doddareddy, H. Choo, Y. S. Cho, K. S. Oh, B. H. Lee and A. N. Pae, *Bioorg. Med. Chem.*, 2009, **17**, 2759–2766; (*b*) J. A. Christopher, P. Bamborough, C. Alder, A. Campbell, G. J. Cutler, K. Down, A. M. Hamadi, A. M. Jolly, J. K. Kerns, F. S. Lucas, G. W. Mellor, D. D. Miller, M. A. Morse, K. D. Pancholi, W. Rumsey, Y. E. Solanke and R. Williamson, *J. Med. Chem.*, 2009, **52**, 3098–3102; (*c*) C. M. Avila, A. B. Lopes, A. S. Goncalves, L. L. da Silva, N. C. Romeiro, A. L. P. Miranda, C. M. R. SantAnna, E. J. Barreiro, C. A and M. Fraga, *Eur. J. Med. Chem.*, 2011, **46**, 1245–1253.
26 Q. L. Guo. Q. D. You, F. Feng and W. Y. Liu, *Chinese Patent*, ZL01008049, 2003.
27 Z. Q. Wu, Q. L. Guo, Q. D. You, L. Zhao and H. Y. Gu, *Biol. Pharm. Bull.*, 2004, **27**, 1769–1774.